

Comprehensive Summaries of Uppsala Dissertations
from the Faculty of Science and Technology 862



Numerical Techniques for Acoustic Modelling and Design of Brass Wind Instruments

BY

DANIEL NORELAND



ACTA UNIVERSITATIS UPSALIENSIS
UPPSALA 2003

Preface. When H. Bouasse published his *Instruments à Vent* in two volumes in 1929–30, he set the starting point for what can be regarded as modern research on musical acoustics. Some 40 years later, the stock of published papers could be counted in their hundreds. However, it is only during the last two or three decades that our physical understanding, in combination with the development of computers, has made it possible to analyse wind instruments with the precision necessary, not only to explain the basic principles of their function, but also to be of practical use for instrument makers. This thesis deals with numerical methods and procedures for the analysis and design of acoustic horns of the kind found in brass instruments. The same models are applicable also to loudspeaker horns, with which one part of the thesis is concerned.

Although the properties and merits of different systems for sound reproduction, such as loudspeakers, are sometimes debated lively, it is at least possible to define an ideal system, in the sense that the sound at the position of the listener's ears should be in as good agreement as possible with the sound at the position of the microphone in the concert hall during the recording.

When speaking about optimisation of musical instruments, one has to be much more careful. The instruments of the modern western orchestra are the result of centuries of evolution, where tradition, musical ideals, performance techniques, and acoustical considerations have been inextricably intertwined with each other. Our judgement about a certain instrument is dependent on a preconception about how the instrument *should* sound [13], and this preconception may vary between individuals, different musical settings and different times. It is important to bear in mind that the term “quality” for the sound of a musical instrument lacks sense, unless one also places the instrument in its musical context.

Nevertheless, research on musical acoustics is of more than constructional interest. Firstly, it gives the possibility to quantify the differences between instruments, and to answer the question why one instrument is considered to be better than another. Secondly, once we have a clear-cut idea about what we expect from an instrument, we can apply the mathematical tools in order to make instruments that comply with our standards as far as possible.

NUMERICAL TECHNIQUES FOR ACOUSTIC MODELLING AND DESIGN OF BRASS WIND INSTRUMENTS

DANIEL NORELAND

1. Introduction.

Inasmuch as one can only judge what is the most agreeable of the sounds of all instruments if he has heard them all and compared them with one another, this has never occurred. And this cannot be done, for we always leave more inventions to posterity which we have not found.

—Marin Mersenne, *Harmonie Universelle I:IV*, 1635.

One of the challenges when modelling musical instruments is the superb capability of the human auditory system to detect subtle differences between sounds. The most basic educational models notwithstanding, a mathematical model of a musical instrument will eventually in some way or another be measured against this system. If the errors of our models are larger than what the ear is capable of detecting, then the models are clearly of limited use. This is one of the biggest—but also one of the most stimulating—difficulties in musical acoustics.

1.1. Physical background. The process governing sound generation in a brass instrument is surprisingly complicated to explain. It is not possible to give a detailed description of brass sound generation here, even for simplified models, but a brief overview is motivated as a background to the concern with impedance functions of brass instruments. For a more thorough description, the reader is referred to a paper by Adachi and Sato [1], and the more general description of wind instrument sound production by Fletcher and Rossing [13].

A sounding brass instrument consists essentially of two components: the instrument itself, and the *lip valve*. The role of the instrument is basically to work as a resonator, in which standing waves of well defined frequencies are built up under the influence of the player's vibrating lips. The term lip valve emphasises the fact that the lips pressed against the mouthpiece constitute a pressure controlled valve, which delivers an airflow whose magnitude depends on the pressure in the oral cavity and in the mouthpiece. The lips of a brass player corresponds to the cane reed in a reed instrument.

The lips are both complex to model and characterised by large variations between different players, but also within the same player during different playing conditions. Nevertheless, simple mass-spring models of the lips have been tried with some success, although work remains to be done, presumably with three-dimensional models of the kind that have been employed for the simulation of vocal cord motion [3].

The lip valve is often described as outward-striking, meaning that the lips

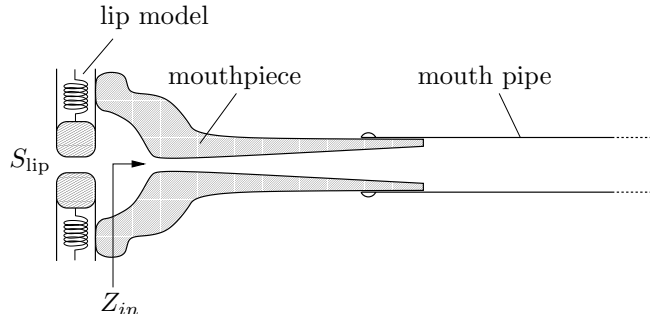


FIG. 1. Mouthpiece and simple mass–spring model of the lip valve.

deform outward due to a pressure increase in the oral cavity, and vice versa for a pressure increase in the mouthpiece. Later investigations have revealed that the situation is not that simple. In the high register, the lip motion is rather transversal, or sideway-striking, like that of two sliding doors. The lip valve is in this case closed solely due to the action of the Bernoulli force, whereas for the outward-striking model, also the static pressure controls the opening. For most playing conditions, the lip vibrations are better described by a combination of the two models [2].

In the following, the simplest of the two lip models is employed, namely the transverse model. It is also assumed that the sound pressure level is low, so that non-linear effects can be neglected in a first approximation. Consider the lip model shown in Fig. 1. The two masses representing the lips are free to move in the vertical direction under the influence of the Bernoulli force, a damping force, and a spring force following Hooke’s law. The area of the lip orifice is denoted S_{lip} . The lip valve system is attached to the instrument, which is essentially nothing but an impedance transformer. If a volume flow velocity $U(\omega)$ is fed into the mouthpiece, a resulting acoustic pressure $p(\omega)$ can be registered at the same place. The relation between the two entities is denoted the *input impedance* of the instrument,

$$p(\omega) = Z_{in}(\omega)U(\omega). \quad (1)$$

The relation between the lip orifice area S_{lip} and the pressure p in the mouthpiece is given by

$$S_{lip}(\omega) = G(\omega)p(\omega). \quad (2)$$

The function $G(\omega)$ is derived by applying Newton’s second law of motion to the mass-spring model of the lips, but it is also possible to measure it experimentally.

The flow between the lips is basically governed by the Navier–Stokes equations. After linearisation, it can be shown that the relationship between U , p and S_{lip} follows the equation

$$U = -c_1p + c_2S_{lip}, \quad (3)$$

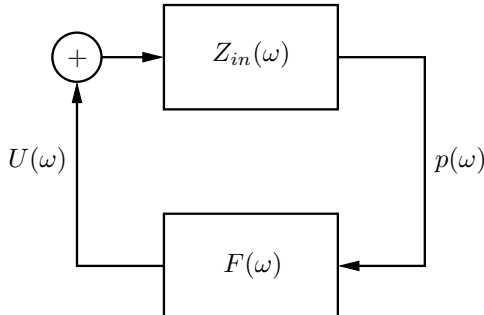


FIG. 2. Block scheme representation of a brass instrument and the lip valve. Z_{in} represents the instrument, and F represents the lip valve

where c_1 and c_2 are positive constants that depend on the pressure in the oral cavity and some other entities. As Eq. (3) shows, the flow through the lip valve decreases with p , but increases with S_{lip} .

Substitution of Eq. (2) into Eq. (3) yields

$$U(\omega) = F(\omega)p(\omega), \quad (4)$$

where $F(\omega) = -c_1 + c_2G(\omega)$. Equations (1) and (4) suggest that the instrument and the player's lips can be viewed as a linear feedback system according to Fig. 2. The requirement for self sustained oscillation of constant amplitude in the feedback system is

$$Z_{in}(\omega)F(\omega) = 1.$$

In order for a strong tone to build up, it is required that

$$|Z_{in}(\omega)F(\omega)| > 1, \quad (5a)$$

$$\arg Z_{in}(\omega) + \arg F(\omega) = 0. \quad (5b)$$

In reality, the amplitude of the oscillations will be limited by non-linearities in the system. As can be observed from Eq. (5a), oscillation is most likely to occur for frequencies where both $|Z_{in}|$ and $|F|$ are large. Eq. (5b) can be satisfied if the frequency is near a maximum of either $|Z_{in}|$ or $|F|$, since here their arguments change rapidly, covering a large range of values. The maxima of $|Z|$ and $|F|$ correspond to the resonance frequencies of the air column in the instrument and of the lip valve itself, respectively. It should be noted that the resonance frequency of the lips can be adjusted considerably by changing the muscle tension. Figure 3 shows an example of what the input impedance of a brass instrument may look like.

The neglected non-linearity is important from other aspects than limiting the sound pressure level. The non-linearity of the lip valve is mainly determined by

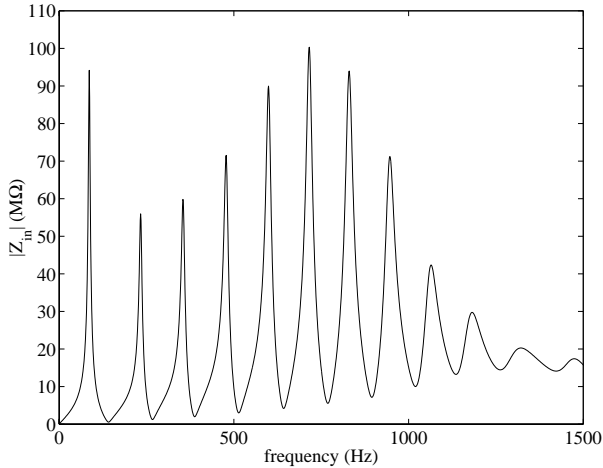


FIG. 3. *Input impedance for a trumpet in Bb with no valves depressed. The frequencies of the playable notes very nearly coincide with the frequencies of the peaks of the spectrum.*

two factors. The first one is the non-linear terms in the Navier–Stokes equation describing the air flow between the lips. The second important non-linear source is if the lips close completely, thus cutting the air flow during part of their vibrational cycle. The effect of the non-linearity is to generate harmonics of the blown notes. These harmonics also affect the action of the lip valve, just as does the fundamental. In order for a note to be clear and stable, it is important that also the harmonics cooperate with the lip vibrations. Therefore, both the fundamental and at least one of its harmonics must correspond to impedance maxima of the air column. This is why it is not practical to design a brass instrument with an arbitrary overtone series. For brass instruments with a considerable length of cylindrical tubing, such as the trumpet and the trombone, the fundamental frequency does not fit into a harmonic series. The corresponding note, which is not regularly used, is considerably wobbly and lacks clarity due to the misalignment between the harmonics of the tone, and the second, third etc. impedance peaks.

1.2. Effects of significance in brass modelling. A question that arises when one is first confronted with the problem of modelling a wind instrument, is how general the description of the physics of the instrument needs to be in order to capture all effects of significance. The required accuracy depends on the purpose of the model. If the intention is to synthesise sound, it is probably correct to say that the demands are less strict than if the model is used for instrument design. As long as a model is good enough to produce a realistic sound, the particular values of the included parameters etc. are of minor concern. Furthermore, a system for sound synthesis must work in real time,

which precludes the use of computationally expensive models. This is not to say that physical modelling is of no use for the sound synthesis community. On the contrary, advanced models make it possible to study the importance of different physical effects in a way that may be difficult to do experimentally. When the effects important for the characteristics of the instrument at hand have been isolated, it is hopefully possible to deduce a simplified and computationally less expensive model for real time sound synthesis.

An indiscriminate description of a musical instrument, considering all physical effects of relevance as equally important throughout the instrument, would require enormous computational resources. First of all, the instrument would be modelled in three dimensions. Secondly, the dynamics of the air in the instrument would be modelled by the Navier-Stokes equation, complete with thin boundary layers near the walls, non-linearities and the associated turbulent flow that possibly appears in the mouthpiece. These effects would require a large number of grid points for the discretisation. Furthermore, the walls of the instrument are not completely rigid, and at least some of the acoustic energy supplied to the air column is transferred to wall vibrations. As stated earlier, the perhaps most unclear component of a brass instrument is the player's lips. Another complex factor is the mouth cavity which imposes a significant acoustic load on the lips. Changing the volume of the mouth cavity affects the sound of a blown note markedly.

Fortunately, a model of the generality mentioned previously is hardly necessary. In the list of examples above, the only somewhat controversial effect is the influence of wall vibrations on the tone of a wind instrument [26]. All the other effects are definitely important. However, they are important in different locations of the instrument, and under different playing conditions. The major part of the plumbing of a brass instrument consists of a rather narrow tube where wave propagation is, to a good approximation, one-dimensional. This is the case also for the duct bends found in most brass instruments. Unless if made very sharp, in which case they may need consideration [18], the bends can usually be treated as if they were straight. The narrow section is also where visco-thermal damping is most significant. This effect is readily included in the analytical solutions that are available for slowly varying, one-dimensional waveguides. In regions of rapid change, such as in the flaring bell, the one-dimensional approximation becomes invalid, which calls for the use of finite-difference, finite-element or boundary-element methods. At the same time, the bell is a part of the instrument with a relatively wide cross section. The large width diminishes the influence of visco-thermal damping, and its inclusion in the model here is not necessary.

1.3. Musically useful horn shapes.

1.3.1. Traditional versus exotic instruments. A common first reaction to the concept of brass optimisation is to ask if the optimisation routines ever yield any new and exotic musical instruments, previously never conceived by

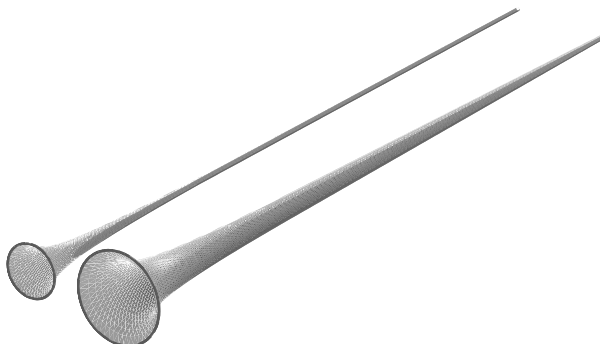


FIG. 4. *Two musical horns representing different brass instrument families. The first eight natural frequencies of the upper horn relate to each other as $0.7, 2, 3, \dots, 8$, whereas for the lower horn, also the fundamental fits into a harmonic sequence. The horn contours are obtained from the numerical shape optimisation algorithms presented in paper V.*

instrument makers. The answer is usually that it depends on what is meant by “exotic”. Starkly wrinkled horn profiles, for instance, are sometimes obtained, but they are usually undesired—even if they satisfy the acoustical demands. If there is a choice between one unorthodox and one more traditionally looking design with essentially the same acoustic properties, the latter is usually preferable. The traditional manufacturing process of brass instruments bells, where a sheet of metal is spun over a mandrel, is impossible to carry out for a bore profile that does not expand monotonically. The modern method of manufacturing bells in sections that are brazed together can of course cope also with contracting horns, should a wavy horn show advantageous. Nevertheless, the cost of producing such a horn would be larger than the cost for a monotonically expanding horn. That being said, also a horn that would be construed as “traditional” by a layman, and possibly by a musician, might be considered as an innovation by an instrument maker. Indeed, musical acoustics is a science of subtleties.

1.3.2. Historical shapes. A historical review of brass instrument development is beyond the scope of this treatise, but is it nevertheless interesting to follow the development of a specific instrument with a long history. Among the wind instruments of the orchestra, the trombone is the instrument that has changed the least since its invention. Developed from the slide trumpet during the late middle ages, the topology of this instrument has remained virtually unchanged since the end of the 15th century. However, in terms of tonal colour and carrying power, the modern trombone is a different instrument¹ from the

¹Something anyone who has tried to play early music with sackbuts replaced by modern trombones has experienced.

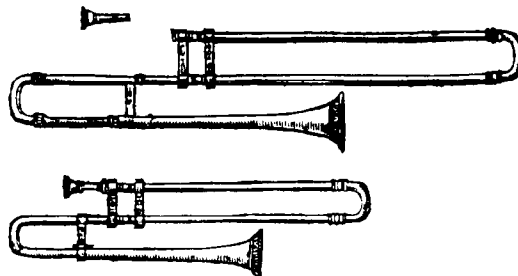


FIG. 5. Early 17th century tenor and alto sackbuts. From Michael Praetorius, *Syntagma Musicum*, Vol. II, *De Organographia*, Wolfenbüttel 1619–20.

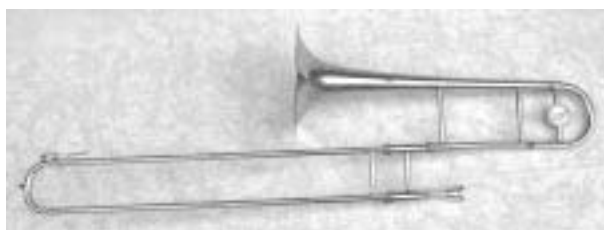


FIG. 6. A modern tenor trombone.

sackbut, its renaissance predecessor. Figure 5 shows the tenor and alto sackbuts depicted in Michael Praetorius' *Syntagma Musicum* from the early 17th century. When compared to the modern tenor trombone of Fig. 6, it is seen that the bell section nowadays constitutes a relatively larger part of the tubing, and has a stronger flare. Less clear from the pictures is that the bore of a modern trombone is considerably wider than in the sackbut. The sackbut had a softer and more mellow tone than its modern descendant—it blended well with the voices of the choir in church music. The modern trombone, in turn, has a more resonant tone with great carrying power, making it the musical fundament of the big band.

1.4. The present state of research on brass acoustics. Although the principles of sound generation in brass instruments are understood in principle, much work remains before the details are unravelled to the extent that it is possible to predict the sound of any brass instrument.

Lip modelling is an active field with on-going work both on the experimental [14] and the theoretical side [19]. As to input impedance analysis, accurate models exist for slowly flaring horns, but there is a lack of versatile tools that incorporate the effects of modal conversion near the mouth of the horns. One of the most promising models here is a multi-modal transmission line model reported in [24] and [4], but questions regarding e.g. the radiation impedance remains to be

solved. There are also few, if any, tools designated particularly for modelling of pipe bends and valves, although commercial finite-element or boundary-element codes do cope with such rather cumbersome geometries. A code by H. L of for the simulation of three-dimensional non-viscous wave propagation in toroidal duct bends has been presented in [23], though. A computationally inexpensive way to account for visco-thermal effects is not trivial, however.

Most investigations on brass tone generation assumes that wave propagation inside the instrument is linear. However, it has been reported [15] that the sound pressure level during fortissimo playing on the trombone can reach 175 dB, which corresponds to an acoustic pressure of 20 kPa. This is clearly outside the range of validity for the linear approximation, and it leads to the formation of shock waves. Realistic sound synthesis of trombones and trumpets must account for this effect in order to produce a realistic timbre over the whole dynamic range.

In spite of the relatively large number of papers treating physical modelling of brass instruments, very little in terms of computational tools for instrument makers does exist. To the author's knowledge, the only code for brass instrument workshops available as of today is BIOS, described in [17] and [6].

Related to the optimisation problem is the bore reconstruction problem, where the bore profile of a musical instrument is reconstructed from its input impedance curve. One of the most successful approaches in this respect is the *layer peeling algorithm* [5], where a deconvolution process is employed in order to identify the horn profile from measurements of the impulse response.

1.5. The papers and their mutual relations. Five papers are included in this thesis. The first one treats the problem of computing the input impedance of a brass instrument with high accuracy. A hybrid method is used, where the different parts of the instrument are analysed using different numerical techniques. For one of the techniques employed, namely the finite-difference time-domain method, non reflecting boundary conditions are imposed on a convex surface. This may under certain circumstances lead to instabilities, something that is investigated more closely in paper II. The hybrid method involves the connection of domains by the use of impedance boundary conditions. A multi-modal generalisation of the impedance boundary condition in paper I, useful when the interface between two domains is placed in a region of modal conversion, is presented in paper III. The application of numerical shape optimisation to acoustic horns is presented in paper IV. The horns are here described by a two-dimensional finite-element model. Brass instrument optimisation is treated in paper V, where the instruments are modelled using the one-dimensional transmission line analogy. The results of the last two papers can, after adaption, be merged into a hybrid optimisation scheme; the one-dimensional model is used to work out an initial design, which is then refined by re-designing the outer part of the flaring bell using the two-dimensional model which accounts also for modal conversion.

2. Summaries of the papers.

2.1. Paper I. The ability to accurately compute the acoustic impedance of waveguides is imperative for the analysis of brass instruments. An established method for such computations is the one-dimensional transmission line analogy [12], wherein the instrument is modelled as a series of short cylinders or truncated cones. This model is fast and accurate for slowly varying parts of an instrument, and it is easy to account for visco-thermal losses. However, the transmission line model fails in the rapidly flaring bell, where the one-dimensional assumption breaks down due to the excitation of higher order radial modes. In spite of being evanescent throughout the horn, these modes may have a significant influence on the input impedance spectrum. Another limitation is the difficulty in modelling the radiation impedance of the instrument. In the outer part of the bell, a model that accounts for three dimensional propagation effects is therefore necessary. Such a model also features an accurate description of the radiation impedance. The objective of this paper is to develop a hybrid method in which the computational domain is partitioned in two different regions, each of which is treated independently with a suitable numerical method. One of the method is formulated in the frequency domain, whereas the other method is formulated in the time domain.

The input impedance can be determined experimentally by measuring the acoustic pressure in response to an input volume flow velocity. Such an experiment can be simulated numerically by solving the lossless scalar wave equation $\partial^2 p / \partial t^2 = c^2 \nabla^2 p$, using the standard second order explicit finite-difference method on an orthogonal, curvilinear grid. By feeding a broad-band signal into the throat of the horn, a high resolution impedance spectrum can be computed. The time evolution of the acoustic pressure $p_{in}(t)$ and the volume flow velocity $U_{in}(t)$ are recorded during the simulation, and after Fourier transformation, the input impedance $Z_{in}(\omega) = p_{in}(\omega) / U_{in}(\omega)$ is calculated.

Wave attenuation due to visco-thermal damping at the boundary of the horn has a significant influence on the input impedance spectrum of a brass instrument. It is entirely possible to include damping in the finite-difference model, but the thin boundary layer associated to the low viscosity of air is costly to resolve numerically. Apart from the large number of points in the vicinity of the boundary, the compressed grid cells call for extremely short time steps in an explicit time marching scheme. Fortunately, the importance of damping diminishes with increasing duct radius. This makes it possible to neglect viscosity in the flaring part of the bell. Figure 7 shows the effect on the frequencies of the impedance peaks due to neglected viscosity in the bell. The maximum peak deviation for the transmission line model is plotted as a function of the position to the right of which the viscosity is set to zero. The curve should be compared to Fig. 8, which shows an estimate [9] of the amount of modal conversion in the bell. Apparently, damping is of subordinate importance where modal conversion starts to be significant.

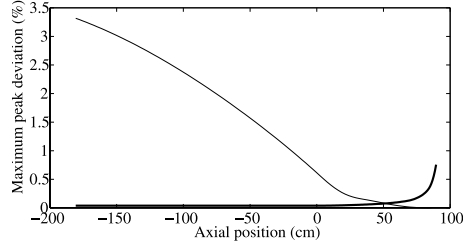


FIG. 7. The effect of neglecting visco-thermal damping in the bell. The horn profile is also indicated for comparison.

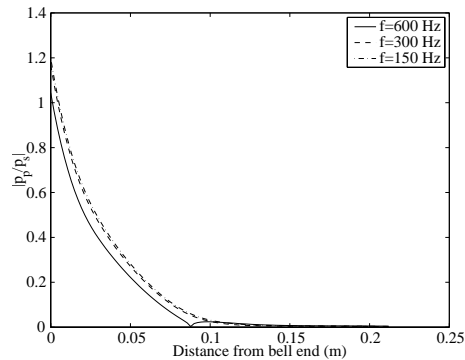


FIG. 8. Estimated mode conversion in the bell.

The geometrical separation between visco-thermal damping and modal conversion suggests the use of a hybrid method, where the bell is analysed separately using the finite-difference method applied on the lossless wave equation. The thus computed input impedance of the bell is then imposed as a load impedance for the rest of the waveguide, which is modelled using the transmission line model, taking losses into account. The partitioning of the instrument is shown in Fig. 9. Figure 10 shows the outer section of a French horn bell embedded in a computational grid. At the horn boundary (denoted by the thick, black curve) the sound-hard boundary condition $\partial p / \partial n$ is imposed. At the outer boundary of the domain, a first order non-reflecting boundary condition is imposed. The particle velocity $\mathbf{v}(t)$, needed for the computation of Z_{in} , is obtained by integrating the linearised momentum balance equation $\rho \partial \mathbf{v} / \partial t = -\nabla p$. In the simulation, the grid resolution and the time step are chosen with respect to the required error tolerance, and the stability condition of the scheme. The complexity of the geometry precludes an *a priori* error estimate, but an estimate of the truncation error of the scheme can be obtained after running the simulation with two different grid resolutions. An initial estimate of the required grid resolution can be obtained by a study of the numerical dispersion of the numerical scheme.

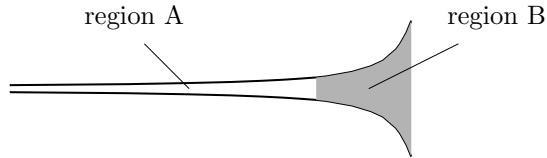


FIG. 9. *Partitioning of the instrument in two domains. Region A is treated using the transmission line model, whereas region B is treated using the finite-difference time-domain method.*

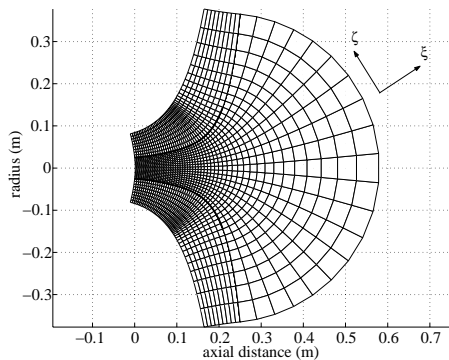
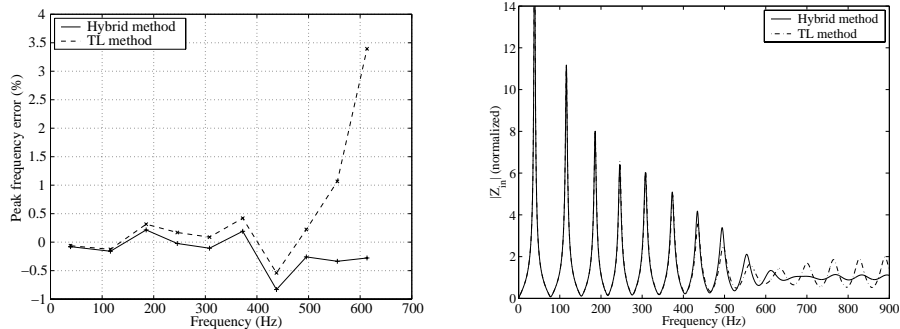


FIG. 10. *Two dimensional grid in a French horn bell corresponding to the shaded region B in Fig. 9*

An experiment was made, where the locations of the impedance peaks for a French horn bell were computed using the hybrid method. The interface between the two methods is placed at a position where visco-thermal damping has become of subordinate importance, but where modal conversion is still low. Figure 11(a) shows the errors in the frequencies of the ten first impedance peaks, for a configuration consisting of a 1.8 m long cylindrical pipe connected to the bell. Also shown are the errors obtained for the transmission line model applied to the whole “instrument”. As can be seen, the two models are equally accurate up to about 500 Hz, where the transmission line model suddenly fails. The hybrid method retains its accuracy, however, since it accounts also for higher modes. A comparison between impedance spectra computed with the transmission line method and the hybrid method is shown in Fig. 11(b). The spectrum of the transmission line method exhibits a persistent series of impedance peaks of considerable magnitude even past the cut-off frequency of the horn [9], where in reality, the horn works effectively as a radiator. This behaviour is typical for the failure on the high frequency side.



(a) Relative error in peak frequency computed by the hybrid method and the transmission line method.

(b) Input impedance spectra computed by the hybrid method and by the transmission line method.

FIG. 11. Results for the pipe-bell configuration. The errors are computed with respect to experimental data.

2.2. Paper II. Absorbing, or non-reflecting, boundary conditions are used in order to model computational domains of infinite extension. In some cases, such boundary conditions may lead to instabilities when applied on boundaries of convex shape. This problem has been observed for perfectly matched layers [25] for electro-magnetic simulations. In the present paper, absorbing boundary conditions for the second order wave equation are shown to be inherently problematic. A simple example from acoustics is given, but the results are applicable also for other wave propagation problems.

Consider the conical waveguide of Fig. 12. A finite difference method is used to simulate wave propagation inside this waveguide. Wave propagation in Ω is governed by the classical wave equation. In the example, only spherically symmetric waves are treated. Initial data to the problem is an acoustic pulse with compact support inside Ω . On the boundary Γ_1 a non-reflecting boundary condition is imposed. A Neumann boundary condition is imposed on the lateral surface Γ_2 . Experiments with three different boundary conditions on Γ_3 are made.

With a Dirichlet condition on Γ_3 , a stable scheme is obtained. The initial pulse is divided into one left- and one right-travelling wave. The left-travelling wave leaves the domain through Γ_1 , as does the other part of the wave after being reflected at Γ_3 . In the case with an absorbing boundary on Γ_3 , both pulses seem to leave the domain, but a closer examination reveals that the scheme allows for a remaining solution component, which is constant in time. In the case with a Neumann condition on Γ_3 , the scheme becomes unstable. Expressed as an eigenvalue problem for the Helmholtz equation, the problem at hand has an

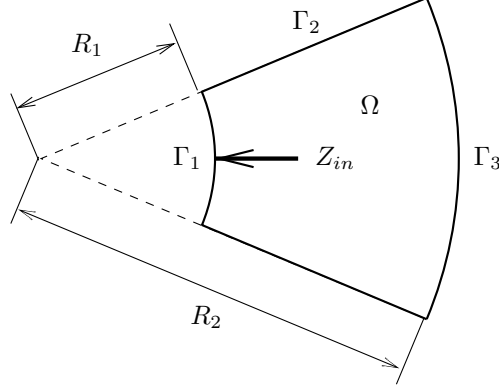


FIG. 12. A converging waveguide.

eigensolution corresponding to a mode with exponential growth in time. This is not feasible from a physical point of view, since the system is assumed to be free from acoustic sources.

An explanation for the instability can be obtained by a study of the fictitious domain *to the left* of Γ_1 . Assuming a time dependence of the form $\exp(i\omega t)$, the spherically symmetric solutions to the wave equation are of the form

$$p(r) = A \frac{e^{-ikr}}{r} + B \frac{e^{ikr}}{r}. \quad (6)$$

Due to the non-reflecting boundary condition on Γ_1 , right-travelling parts of the solution are cancelled, implying that $A = 0$. Under this assumption, and with $B = 1$, the radial component of the particle velocity corresponding to Eq. (6) is given by

$$v(r) = -\frac{1}{\rho c} \frac{e^{ikr}}{r} - \frac{i}{\rho \omega} \frac{e^{ikr}}{r^2}. \quad (7)$$

The boundary condition on Γ_1 can be represented by an impedance boundary condition $Z_{in}(\omega)$, which is defined as the ratio between the acoustic pressure and the volume flow velocity with respect to an inward pointing normal;

$$Z_{in}(\omega) = -\left. \frac{p}{Sv} \right|_{\Gamma_1} = \frac{\rho c}{S} \frac{i\omega}{i\omega - \frac{c}{R_1}},$$

where S is the area of Γ_1 . Restricting the argument to causal systems, but allowing for exponentially growing signals, it is convenient to work with the unilateral Laplace transform. In this case we have

$$\tilde{Z}_{in}(s) = \frac{\rho c}{S} \frac{s}{s - \frac{c}{R_1}}. \quad (8)$$

The input impedance, which can be seen as the transfer function from $U(\omega)$ to $p(\omega)$ at Γ_1 , has a pole with positive real part. (A derivation of the impedance corresponding to an absorbing concave boundary condition, e.g. on Γ_3 , would yield an expression similar to Eq. (8), but with the pole instead in the left half plane.) A system whose transfer function has a pole in the right half plane is known to be unstable. Accordingly, the impulse response given by the inverse Laplace transform of \tilde{Z}_{in} ,

$$h(t) = \mathcal{L}^{-1}\tilde{Z}_{in}(s) = \frac{\rho c}{S} \left(\delta(t) + \frac{c}{R_2} e^{ct/R_1} \Theta(t) \right),$$

where $\Theta(t)$ denotes the Heaviside step function, is exponentially growing. This is a consequence of the non-physical assumption that converging waves can be passively absorbed in the tip of a cone without reflection. Whether a convex absorbing boundary condition really leads to instability in a real case depends on the other boundary conditions of the problem.

2.3. Paper III. Impedance boundary conditions (IBC) are a means of connecting different sub-regions of a computational domain when solving wave propagation problems in the frequency domain. An IBC is an integral operator, over the surface of a computational domain, that relates the solution to its normal derivative. This paper treats the problem of an acoustic waveguide with a step discontinuity, and how it can be represented by an IBC.

There can be several reasons for separating the computational domain in parts treated independently. The whole domain may be too large to be treated as is, different numerical methods may be required on the various parts, or it may be the case that each region is analysed and stored in a library of building blocks for later retrieval.

Consider the waveguide in Fig. 13. Wave propagation in $\Omega = \Omega_l \cup \Omega_r$ is modelled by the Helmholtz equation $\Delta p + k^2 p = 0$, $\partial p / \partial n = 0$ at $\partial\Omega$. Assume that a wave coming from the left is incident in the step discontinuity at $x = 0$. As a result, the incoming wave is partially reflected and partially transmitted into the narrower part $x > 0$. The wave field in the vicinity of the step is much more complicated than some distance away from $x = 0$. This is a common scenario in many real-world applications in acoustics. Nevertheless, it is the far-field solution that is of most interest, simply because the near-field effects are very local. The near field region occupies typically no more than a few wavelengths, or maybe only a fraction of a wavelength. The local effects do, however, have an influence on the far-field solution. When applying numerical techniques for the waveguide in Fig. 13, a fine resolution is therefore needed for the local wave phenomena in the vicinity of $x = 0$. At the same time, a much coarser discretisation is enough just a short distance away from $x = 0$. One way to deal with this problem is to use adaptive grid refinement. In this paper, a different technique is suggested. The domain is divided into the two parts $x \leq -L$ and $x > -L$, $L > 0$, where $x = -L$ is a fictitious boundary. The two domains may be treated entirely

independently of each other using different numerical methods and/or different grids. For the domain $x \leq -L$, an IBC is created at $x = -L$ which simulates the wave response of the step discontinuity. It is shown that the number of degrees of freedom in this IBC diminishes as the distance to $x = 0$ is increased. The construction of the IBC entails the solution of the wave propagation problem around $x = 0$, and this has to be carried out using a high resolution. The IBC at $x = -L$ is thus an aid to tie domains together, which require vastly different computational work for the solution of the underlying equation. This paper illustrates this approach for the simple geometry of Fig. 13. Using separation of variables, the solution to the Helmholtz equation can be expressed in terms of modal expansions of the form

$$p(x, y) = \sum_n P_n(x) \varphi_n(y), \quad (9)$$

to the left and to the right of $x = 0$, respectively. The expansion coefficients are derived by stating Eq. (9) in terms of right and left travelling waves. An equation for the unknown coefficients is then formed requiring continuity condition of the solution and its gradient at $x = 0$, and fulfilment of the boundary condition $\partial p / \partial n = 0$ along the vertical boundary. This is the so-called mode matching technique. For numerical computation, the number of modes in the expansions must be finite. Furthermore, the ratio between the number of modes to the left and to the right must correspond to the ratio between the characteristic sizes of the waveguide [21]. With this choice, second order convergence for the expansion coefficients can be verified, as the number of expansion terms increases.

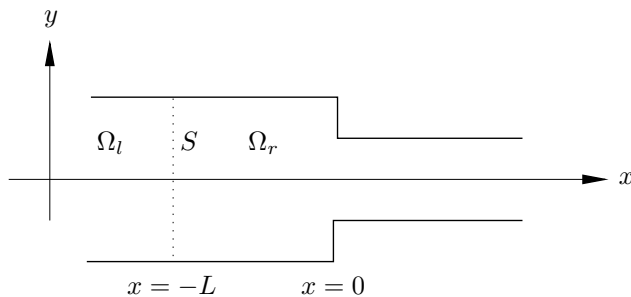


FIG. 13. Channel with a step discontinuity.

The acoustic response of the part of Ω for which $x \leq -L$, is contained in the impedance matrix \mathbf{Z}_L , defined by the relation

$$\mathbf{P} = \mathbf{Z}_L \frac{\partial}{\partial x} \mathbf{P}, \quad \mathbf{P} = (P_0, P_1, \dots, P_N)^T.$$

The elements of \mathbf{Z}_L describe the coupling between the modes and their normal derivatives at the fictitious boundary S . Elements corresponding to the cross

coupling between different modes, of which at least one is evanescent, go to zero as the distance to the discontinuity is increased. It is therefore sufficient to include only a few number of modes in the IBC, when applying it some distance away from $x = 0$. In the far field limit, only the propagating modes need be considered, but it is usually desirable to place the boundary closer to the discontinuity in order to reduce the size of the computational domain. This consideration is relevant if the Helmholtz equation is solved using a discrete method, in which case the region in the vicinity of the discontinuity may need a finer discretisation than the rest of the domain. Figure 14 shows the relative error in the principal mode of the back-reflected field when an IBC is placed at different positions $x = -L$. It can be seen that the accuracy improves as the distance L , and the number of degrees of freedom increases. $L = -0.5$ is around one quarter of a wavelength, which implies that the sound field can be computed using a quite modest resolution only a short distance away from $x = 0$. As the figure also shows, at least as many modes must be included in \mathbf{Z}_L , as there are propagating modes.

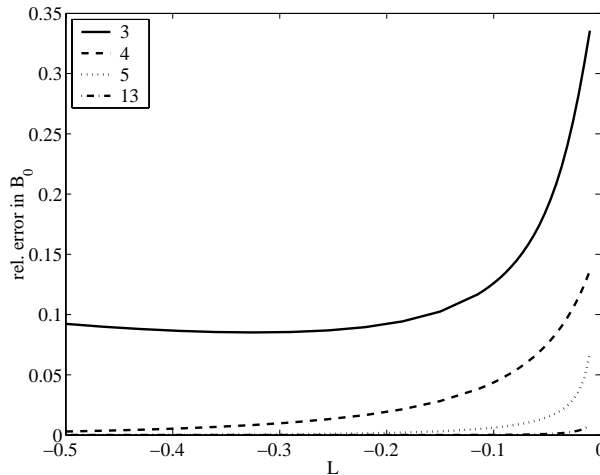


FIG. 14. *Error in planar mode reflection coefficient. The frequency allows for four propagating modes.*

2.4. Paper IV. Acoustic horns are important devices in applications such as loudspeakers and musical instruments, where they are used as impedance transformers to the surrounding air. This paper treats the problem of designing a loudspeaker horn that provides an optimal impedance match between a waveguide and the surrounding air. The aim of the matching is to impose a high acoustic resistance on the loudspeaker diaphragm, so that maximum power is supplied to the surrounding air. Without such matching, the diaphragm may

move vigorously, but if the movement is done against a low acoustic pressure, very little energy is transferred out of the loudspeaker. The objective of this paper is to optimise the transmission efficiency of an acoustic horn. A measure of the quality of the horn is therefore the part of the energy incident on the horn from the diaphragm that is reflected back, and not transmitted out from the horn. This reflection should be minimised.

The paper addresses mainly two issues of shape optimisation. The first question regards the formulation of a fast optimisation algorithm. A gradient based library routine is used to solve the minimisation problem. The routine requires a computationally inexpensive and accurate gradient of the objective function, which is here derived using an adjoint equation technique formulated for the discrete numerical scheme describing wave propagation in the horn.

The second issue concerns how the optimiser can be made to find geometrically feasible shapes. A common problem for many shape optimisation algorithms is the propensity for developing irregular shapes. This difficulty is tackled by letting the horn contour be defined as the solution to a Poisson equation. By optimising with respect to the right hand side of this equation, it is shown that the obtained shapes are much smoother than if optimisation is carried out directly with respect to the contour shape.

The geometry of interest is shown in Fig. 15. It is a half model of an acoustic horn and a portion of the region of air surrounding it. The horn is of infinite extension in the z -direction, which effectively reduces the problem to two dimensions. Wave propagation inside and outside the horn is modelled by the scalar Helmholtz equation. At the walls of the horn, the sound-hard boundary condition $\partial p / \partial n$ is imposed. This boundary condition is also imposed on the symmetry plane of the geometry. In order to simulate an infinite space around the horn, a first order, non-reflecting Engquist–Majda boundary condition is imposed on Γ_{out} . This radiation boundary is placed in the acoustic far-field region, where wave propagation is approximately cylindrical. Finally, a variant of an absorbing boundary condition is imposed on Γ_{in} . It prescribes a planar wave of amplitude A that enters the channel, but allows for left travelling waves to leave the channel. With notations according to Fig. 15, the mathematical model is

$$c^2 \Delta p + \omega^2 p = 0 \quad \text{in } \Omega, \quad (10a)$$

$$(i\omega + \frac{c}{2R_\Omega})p + c \frac{\partial p}{\partial n} = 0 \quad \text{on } \Gamma_{\text{out}}, \quad (10b)$$

$$i\omega p + c \frac{\partial p}{\partial n} = 2i\omega A \quad \text{on } \Gamma_{\text{in}}, \quad (10c)$$

$$\frac{\partial p}{\partial n} = 0 \quad \text{on } \Gamma_n \cup \Gamma_{\text{sym}}. \quad (10d)$$

By decomposing the sound field in the channel in right and left travelling waves so that $p(x) = A \exp(-ikx) + B \exp(ikx)$, the power output is maximised

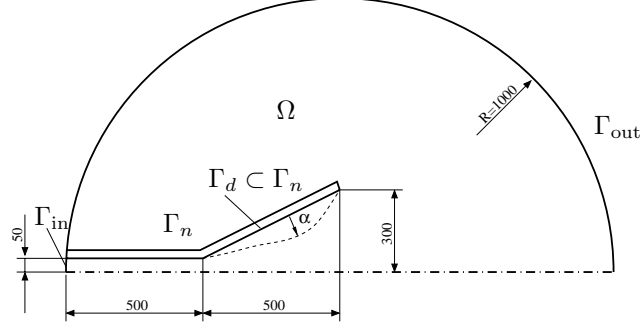


FIG. 15. Computational domain for a horn optimisation problem. The design boundary Γ_d is part of Γ_n .

when B is minimised. This suggests the objective function

$$J(\eta) = \frac{1}{2} \int_{\Gamma_{\text{in}}} |p(\eta) - A|^2 d\Gamma. \quad (11)$$

Optimisation is carried out by varying the shape of the design boundary Γ_d . The set of admissible designs is defined as deflections in the normal direction \mathbf{n}_{ref} from the reference design;

$$\Gamma_d = \{\mathbf{x} | \mathbf{x} = \mathbf{x}_{\text{ref}} + \alpha(\mathbf{x}_{\text{ref}})\mathbf{n}_{\text{ref}}, \quad \mathbf{x}_{\text{ref}} \in \Gamma_d^{\text{ref}}\}.$$

As a means to avoid intermediate wiggly designs of Γ_d , $\alpha : \Gamma_d^{\text{ref}} \rightarrow \mathbb{R}$ is required to be the solution to

$$\begin{aligned} -\alpha'' &= \eta \quad \text{on } \Gamma_d^{\text{ref}} \\ \alpha &= 0 \quad \text{at the end points of } \Gamma_d^{\text{ref}}, \end{aligned}$$

where η is the design variable with respect to which the optimisation is done.

The optimisation problem (11) is solved using the BFGS quasi-Newton algorithm. The following method is used to compute the gradient $\nabla_{\eta} J$; Given the solution p to state equation (10), solve the *adjoint equation*

$$c^2 \Delta z + \omega^2 z = 0 \quad \text{in } \Omega, \quad (12a)$$

$$\left(-i\omega + \frac{c}{2R}\right)z + c \frac{\partial z}{\partial n} = 0 \quad \text{on } \Gamma_{\text{out}}, \quad (12b)$$

$$-i\omega z + c \frac{\partial z}{\partial n} = p - A \quad \text{on } \Gamma_{\text{in}}, \quad (12c)$$

$$\frac{\partial z}{\partial n} = 0 \quad \text{on } \Gamma_n \cup \Gamma_d \cup \Gamma_{\text{sym}}. \quad (12d)$$

Then compute

$$\nabla_{\alpha} J = \gamma \text{Re}(\omega^2 \bar{z}_{\alpha} p_{\alpha} - c^2 \nabla \bar{z}_{\alpha} \cdot \nabla p_{\alpha}), \quad (13)$$

where γ is a metric term, and where p_α and z_α are observations of p and z along Γ_d . $\nabla_\eta J$ is finally obtained as the solution r to the Poisson problem

$$-r'' = \nabla_\alpha J \quad (14)$$

$$r = 0, \quad \text{at the end points of } \Gamma_d^{\text{ref}}. \quad (15)$$

Discretised versions of Eq. (10) and Eq. (11) are obtained by applying a finite-element method to Eq. (10). The discrete adjoint equation is then derived from the discrete forward problem. The solution p depends on Γ_d through the positions of the grid points of the mesh. This necessitates differentiation of the solution to a finite-element problem with respect to the nodal coordinates of the mesh. Changes in the shape of Γ_n induce displacements of the interior nodes. The distribution of these changes follow an equation from linear elasticity. The algorithm for computing the gradient is exact, and in computational terms considerably more inexpensive than finite-differencing.

For practical purposes, the objective function is defined as a sum of terms of the kind in Eq. (11), each of them referring to one of a number of frequencies in the design frequency band.

Figure 16(a) shows the initial shape, and the optimised shape for an experiment with 27 equally distributed frequencies between 310 Hz and 705 Hz. The reflection spectrum is shown in Fig. 16(b). The amplitude of the reflection from the horn is less than 0.5 % throughout the design frequency band. It is not possible to perform this optimisation without the use of smoothing, or some other method for prevention of irregular designs. Conclusively, our algorithm is at the same time efficient in computational terms, and successful in finding smooth solutions that satisfy the acoustic requirements.

2.5. Paper V. This paper treats the problem of optimising the intonation of brass instruments using gradient based minimisation routines. The task entails the adjustment of a number of peaks in an impedance spectrum by variation of the shape of the instrument. Three major difficulties are encountered in this process: the formulation of a suitable objective function, the implementation of a fast forward solver that can be differentiated with respect to the design parameters, and the prevention of the optimisation process from getting stuck in local minima corresponding to undesired shapes.

The instruments are considered to be straight and moderately flaring, so that they can be modelled accurately using a one-dimensional transmission line analogy based on waveguide sections shaped as truncated cones, as in Fig. 17. Denoting by \mathbf{H} the transfer matrix of the instrument, defined through the relation

$$\begin{bmatrix} p_{in} \\ U_{in} \end{bmatrix} = \mathbf{H} \begin{bmatrix} p_L \\ U_L \end{bmatrix} = \begin{bmatrix} H_{11} & H_{12} \\ H_{21} & H_{22} \end{bmatrix} \begin{bmatrix} p_L \\ U_L \end{bmatrix} \quad (16)$$

between the acoustic pressure and volume flow at the ends of the instrument,

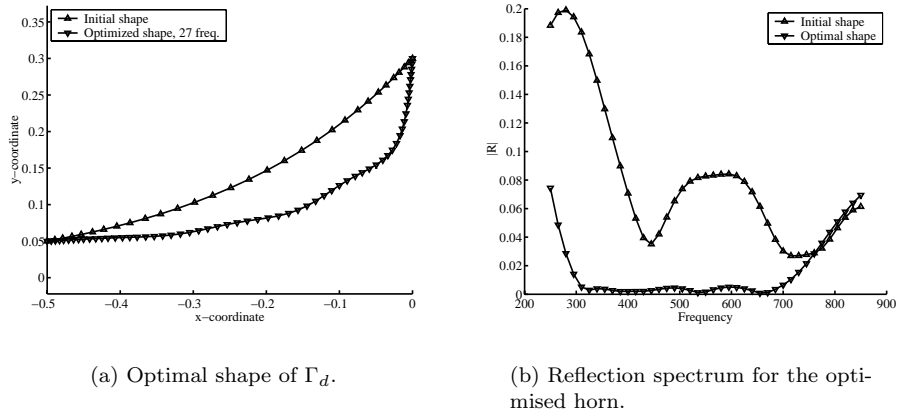


FIG. 16. Optimisation for 27 frequencies in the interval 310 Hz to 705 Hz.

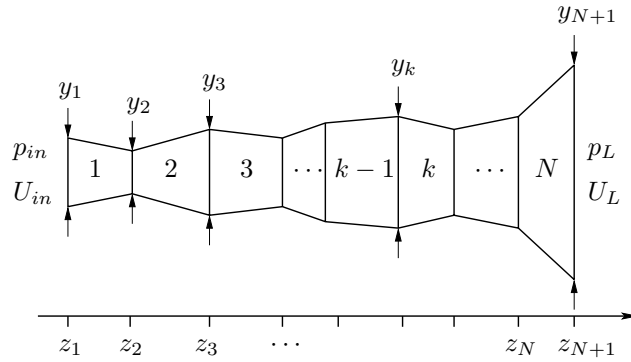


FIG. 17. A horn approximated as a series of truncated cones.

the input impedance is given by

$$Z_{in} = \frac{H_{12} + H_{11}Z_L}{H_{22} + H_{21}Z_L}, \quad (17)$$

where Z_L is the radiation impedance. \mathbf{H} is approximated by the product of the transfer matrices of the short conical sections [20],

$$\mathbf{H} = \prod_{j=1}^N \mathbf{H}_j(y_j, y_{j+1}, z_j, z_{j+1}). \quad (18)$$

An expression according to Beranek [10] is used to approximate Z_L .

A measure of the intonation and response of a wind instrument is given by the locations and magnitudes of the peaks of its input impedance spectrum [8]. Sharp peaks at the intended resonance frequencies are usually desired. The argument of Z_{in} is, to a good approximation, zero at the impedance peaks, which suggests the objective function

$$J(\boldsymbol{\alpha}) = \frac{1}{2} \sum_{k=1}^n [\text{Im}(Z_{in}(f_k))^2 + \text{Re}(Z_{in}(f_k) - Z_{\text{peak}_k})^2], \quad (19)$$

where $\boldsymbol{\alpha} \in \mathbb{R}^m$ is the set of design variables, f_k , $k = 1, \dots, n$ are the desired peak frequencies, and Z_{peak_k} , $k = 1, \dots, n$ are the corresponding peak levels. Formulated as a non-linear least-squares problem, minimisation of Eq. (19) corresponds to the problem

$$\boldsymbol{\alpha}_* = \arg \min_{\boldsymbol{\alpha} \in \mathbb{R}^m} J(\boldsymbol{\alpha}) = \arg \min_{\boldsymbol{\alpha} \in \mathbb{R}^m} \frac{1}{2} \mathbf{F}^T \mathbf{F}, \quad (20)$$

where \mathbf{F} is commonly denoted the *residual*, here given by

$$\mathbf{F} = \begin{bmatrix} \text{Im}(Z_{in}(f_1)) \\ \text{Re}(Z_{in}(f_1) - Z_{\text{peak}_1}) \\ \text{Im}(Z_{in}(f_2)) \\ \text{Re}(Z_{in}(f_2) - Z_{\text{peak}_2}) \\ \vdots \end{bmatrix}. \quad (21)$$

Earlier work on brass optimisation [16] has employed genetic algorithms and the zero order Rosenbrock minimisation algorithm, which are robust but converge slowly. In order to attain faster convergence, the minimisation of the objective function is in this work performed using the Levenberg-Marquardt algorithm. This is a combined Gauss–Newton and trust region method that has been used successfully for many different non-linear least-squares problems. The necessary gradient $\nabla_{\mathbf{y}} J$ requires differentiation of Z_{in} with respect to the end diameters y_k , $k = 1, \dots, N + 1$. This differentiation is carried out by symbolic manipulation of Eq. (17), which in turn requires differentiation of \mathbf{H} . From the product rule applied to Eq. (18), a succession of cumulative products are necessary in order to evaluate $\partial \mathbf{H} / \partial y_k$, $k = 1, \dots, N + 1$. These products are computed and stored prior to the gradient evaluation, which makes the process computationally inexpensive.

As in [7], some provision has to be made against the development of irregular designs. To this end, two methods were tried: constraining the search space through a parametrisation of the geometry, and smoothing. The parametrical description has as unknowns a few number of parameters in a function describing the bell profile, and the length of a piece of cylindrical or conical main tubing attached to the bell. Figure 18 shows the shape obtained in an attempt to design an instrument with eight harmonically related resonance frequencies.

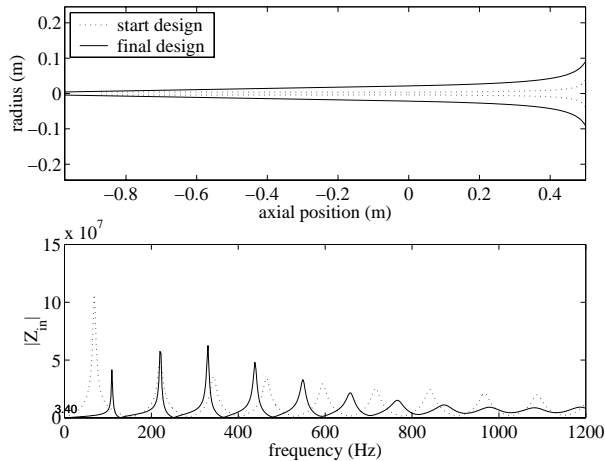


FIG. 18. Harmonic instrument constructed of a Bessel horn attached to a conical pipe.

With smoothing of the same kind as in [7], the number of design parameters is retained, but the optimiser is given a preference for smooth design updates. Some means of increasing the convergence radius of the optimisation may be necessary in order to deal with large deformations from the initial design. A method is suggested, where impedance peak frequency and magnitude are treated in separate steps. In order to test this approach, a typical brass instrument bell was analysed with respect to its first nine impedance peaks. Starting from an initial design shaped as a truncated cone with the same length and end diameters as the original horn, the aim was then to reproduce the shape of the bell by matching the frequencies and the magnitudes of the impedance peaks. The resulting design, which is remarkably close to the original bell, is shown in Fig. 19. In 121 iterations, the loss function has converged to zero within computational precision. The number of components in the residual in this experiment was 18, and the number of design parameters was 100. Since the problem is under-determined, it has several solutions. Whether or not all of these are close to each other in the L^2 sense, or if there are also other very different designs that yield a zero residual remains an open question.

Two different instruments with the same acoustic properties are not necessarily equally good from a manufacturer's perspective. An optimisation problem is therefore formulated, where the smoothness of the instrument is optimised, treating intonation as a constraint. The loss function $j(\eta)$ measuring the smoothness is here essentially defined as

$$j(\eta) = \int_0^a (y''(z))^2(z) dz, \quad (22)$$

whereas the definition of the intonations constraint is akin to Eq. (21). The

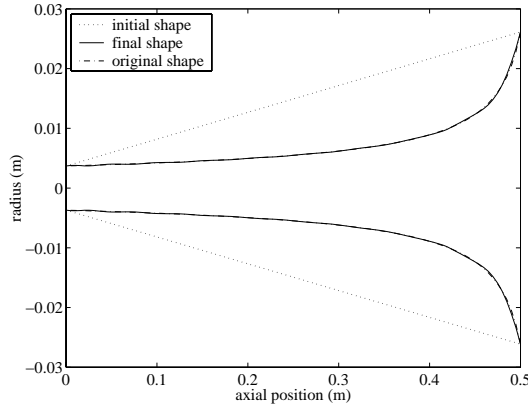


FIG. 19. Original shape, and the shape obtained after optimisation considering the frequencies and magnitudes of the nine first impedance peaks.

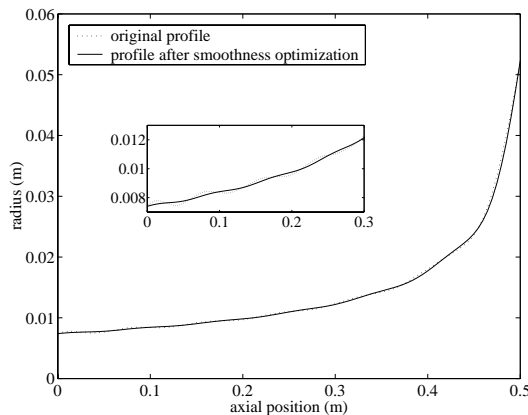


FIG. 20. Horn shapes before and after smoothness optimisation. The frequencies and magnitudes of the six first impedance peaks are the same for both horns, but after optimisation, a considerably smoother design has been obtained. The inset shows a magnification of the lead pipe.

evaluation of $j(\eta)$ and its gradient is trivial. The constraint, however, is strongly nonlinear and costly to compute. Figure 20 shows results from a smoothness optimisation experiment. The ripples of the horn contour have been reduced significantly, if not disappeared completely.

3. Conclusions and future perspectives. The main thread of this thesis is the use of hybrid methods. Real-world physical problems are complex, and it is rare that one single numerical technique is optimal for a whole computational domain, and under every circumstances. If different phenomena are es-

entially localised to different parts of the domain, it is advantageous to perform a domain decomposition, and to apply different methods on the different sub-domains. This necessitates some means of connecting the results again during some stage of the computation. In this work, the connection has been performed using impedance boundary conditions. Utilised in paper I, they are manifested and generalised in paper III. The last two papers approach the horn optimisation problem using different physical models (the transmission line model and the finite-element model). The physical merits of the finite-element model are largely similar to those of the finite-difference model in paper I. This leads to the possibility of unifying the results of paper IV and paper V into a hybrid optimisation scheme.

The work of this thesis has shown that many of the subtle but important effects of wave propagation in the instrument can be accounted for in numerical algorithms, that are reasonable in terms of computational cost. This is a prerequisite for the algorithms to be of use for instrument makers, especially when the algorithms are put in the inner loop of an optimisation process.

The optimisation problems formulated in this thesis are local, which implies that they are best suited for finding shapes close to the initial design, that is to improve existing instruments. Although successful experiments with optimisation “from scratch” have been demonstrated, the gradient based algorithm probably needs to be combined with global methods in order to tackle such tasks in a more systematic way.

There are important applications to duct acoustics other than musical instruments. Closely related is the theory of mufflers [22], which shares many of the features of wind instruments. Another application—dual to musical acoustics in the sense that the intention is to *prevent* the forming of sound—is the construction of noiseless ventilation systems. Such systems consist of long ducts where complicated resonance patterns may occur. The wide cross sections of ventilation ducts allow for several propagating modes, which calls for the use of multi-modal impedance boundary conditions in their modelling.

The problem of horn optimisation has also attracted much interest from the electro-magnetic community. Micro-wave antennas for various applications are often built in the shape of horns. Although the Maxwell equations and the acoustic wave equation are different, they are both hyperbolic systems describing wave propagation. Many results of this thesis should therefore, *mutatis mutandi*, be relevant also for the problem of horn antenna design.

REFERENCES

- [1] S. Adachi and M. Sato. Time-domain simulation of sound production in the brass instrument. *J. Acoust. Soc. Am.*, 97:3850–3861, 1995.
- [2] S. Adachi and M. Sato. Trumpet sound simulation using a two-dimensional lip vibration model. *J. Acoust. Soc. Am.*, 99:1200–1209, 1996.
- [3] A. Alipour, D.A. Berry, and I.R. Titze. A finite-element model of vocal-fold vibration. *J. Acoust. Soc. Am.*, 108:3003–3012, 2000.

- [4] N. Amir, V. Pagneux, and J. Kergomard. A study of wave propagation in varying cross-section waveguides by modal decomposition. Part II. Results. *J. Acoust. Soc. Am.*, 101:2504–2517, 1997.
- [5] N. Amir, G. Rosenhouse, and U. Shimony. A discrete model for tubular acoustic systems with varying cross section - The direct and inverse problems. parts 1 and 2: Theory and experiment. *Acustica*, 81:450–474, 1995.
- [6] P. Anglmayer, W. Kausel, and G. Widholm. A computer program for optimization of brass instruments. Part II. applications, practical examples. In *Forum Acusticum*, Berlin, 1999.
- [7] E. Bängtsson, D. Noreland, and M. Berggren. Shape optimization of an acoustic horn. *Computer Methods in Applied Mechanics and Engineering*, 192:1533–1571, 2003.
- [8] A.H. Benade. *Fundamentals of Musical Acoustics*. Dover Publications, New York, 1990.
- [9] A.H. Benade and E.V. Jansson. On plane and spherical waves in horns with nonuniform flare. I. theory of radiation, resonance frequencies, and mode conversion. *Acustica*, 31:79–98, 1974.
- [10] L. Beranek. *Acoustics*. McGraw-Hill, New York, 1954.
- [11] H. Bouasse. *Instruments à Vent*. Librairie Delagrave, Paris, 1929–30.
- [12] R. Caussé, J. Kergomard, and X. Lurton. Input impedance of brass musical instruments—Comparison between experiment and numerical models. *J. Acoust. Soc. Am.*, 75:241–254, 1984.
- [13] N.H. Fletcher and T.D. Rossing. *The physics of musical instruments*. Springer, New York, 1998.
- [14] J. Gilbert, S. Ponthus, and J.-F. Petiot. Artificial buzzing lips and brass instruments: Experimental results. *J. Acoust. Soc. Am.*, 104:1627–1632, 1998.
- [15] A. Hirschberg, J. Gilbert, R. Msallam, and A.P.J. Wijnands. Shock waves in trombones. *J. Acoust. Soc. Am.*, 99:1754–1758, 1996.
- [16] W. Kausel. Bore reconstruction from measured acoustical input impedance; equipment, signal processing, algorithms and prerequisites. *Proceedings of the International Symposium on Musical Acoustics*, 2:373–378, 2001.
- [17] W. Kausel, P. Anglmayer, and G. Widholm. A computer program for optimization of brass instruments. part i. concept, implementation. In *Forum Acusticum*, Berlin, 1999.
- [18] D.H. Keefe and A.H. Benade. Wave propagation in strongly curved ducts. *J. Acoust. Soc. Am.*, 74:320–332, 1982.
- [19] D.O. Ludwigsen and W.J. Strong. Normal modes of a finite element lip reed model. *J. Acoust. Soc. Am.*, 109:2483, 2001.
- [20] D. Mapes-Riordan. Horn Modeling with Conical and Cylindrical Transmission-Line Elements. *J. Audio Eng. Soc.*, 41:471–483, 1993.
- [21] R. Mittra, T. Itoh, and T. Li. Analytical and numerical studies of the relative convergence phenomenon arising in the solution of an integral equation by the moment method. *IEEE Transactions on microwave theory and techniques*, MTT-20(2):96–104, 1972.
- [22] M.L. Munjal. *Acoustics of ducts and mufflers*. John Wiley and Sons, 1987.
- [23] D. Noreland and H. Löf. A three dimensional finite difference method for the analysis and design of brass instruments. In *Proc. of the International Symposium on Musical Acoustics*, pages 501–504, Perugia, Italy, Sept 2001.
- [24] V. Pagneux, N. Amir, and J. Kergomard. A study of wave propagation in varying cross-section waveguides by modal decomposition. Part I. Theory and validation. *J. Acoust. Soc. Am.*, 100:2034–2048, 1996.
- [25] F.L. Teixeira. Conformal PML-FDTD schemes for electromagnetic field simulations: A dynamic stability study. *IEEE Transactions on antennas and propagation*, 49(6):902–907, 2001.
- [26] J.W. Whitehouse, D.B. Sharp, and N.D. Harrop. The use of laser doppler velocimetry in the measurement of artificially induced wall vibrations in a wind instrument. In *Proc. of the Institute of Acoustics*, Salford, UK, March 2002.